Multi Satellite Observation of a Foreshock Bubble Causing an Extreme Magnetopause Expansion

Niklas Grimmich[1], Fabio Prencipe[1], Drew L. Turner[2], Terry Z. Liu[3], Ferdinand Plaschke[1], Martin O. Archer[4], Rumi Nakamura[5], David G. Sibeck[6], Johannes Z. D. Mieth[1], Hans-Ulrich Auster[1], Dragos Constantinescu[1], David Fischer[5], Werner Magnes[5]

[1]Institut für Geophysik und Extraterrestrische Physik, Technische Universität Braunschweig, Braunschweig, Germany
[2]Johns Hopkins University Applied Physics Laboratory, Laurel, Maryland, USA
[3]Department of Earth, Planetary, and Space Sciences, University of California, Los Angeles, California, USA
[4]Department of Physics, Imperial College London, London, UK
[5]Space Research Institute, Austrian Academy of Sciences, Graz, Austria
[6]NASA Goddard Space Flight Center, Greenbelt, Maryland, USA

Key Points:

- Multi satellite observation of a large Foreshock Bubble (FB) hitting Earth's magnetosphere.
- The transverse ($y-z$) scale size of the FB can be constrained from observations to be at least 8-10 R_E fitting with simulations.
- Response of the magnetosphere seems to stem from a combination of the size and its motion across the dayside magnetosphere region.

Corresponding author: Niklas Grimmich, n.grimmich@tu-braunschweig.de

Abstract

The interaction of a solar wind discontinuity with the backstreaming particles of the Earth's ion foreshock can generate hot, tenuous plasma transients such as foreshock bubbles (FB) and hot flow anomalies (HFA). These transients are known to have strong effects on the magnetosphere, distorting the magnetopause (MP), either locally during HFAs or globally during FBs. However, previous studies on the global impact of FBs have not been able to determine whether the response stems directly from the transverse scale size of the phenomenon or its fast motion over the magnetosphere. Here we present the observation of an FB and its impact on the magnetosphere from different spacecraft scattered over the dayside magnetosphere. We are able to constrain the size of the transverse scale of an FB from direct observations to be about 10 R_{E}. We further suggest that a combination of this scale and the motion of the FB over the MP is responsible for the previously reported global response of the dayside magnetosphere.

Plain Language Summary

The solar wind is a fast plasma flow of charged particles originating from the Sun. Earth's magnetic field diverts this flow around the planet forming the magnetosphere. The bow shock forms upstream of Earth to decelerate the solar wind and initialize the flow around Earth's magnetic field. A fraction of the solar wind particles are reflected back into the solar wind stream, forming the ion foreshock. In this region interactions between discontinuities in the solar wind and the backstreaming ions can cause transient phenomena with enclosed hot and tenuous plasma called foreshock bubbles (FBs) or hot flow anomalies (HFAs). These transients are convected with the solar wind, interacting with the bow shock and leading to an expansion of the magnetosphere due to lower pressure associated with the transients' core. Such a response was reported before in different studies which conclude that FBs have a global impact on the magnetosphere. In our study we report on another FB observed by a multi-spacecraft constellation. The observations allowed us to constrain the size of the FB in cross-flow dimensions, and we observe that the global response of the magnetosphere happens due to both size and motion of the FB across the bow shock.

1 Introduction

Earth's bow shock (BS) mainly decelerates and diverts the incoming solar wind around the magnetosphere. However, a fraction of the solar wind particles are reflected at the BS and stream along the interplanetary magnetic field (IMF) back into the solar wind. The interactions between this back streaming and the solar wind particles excite plasma waves in the so called foreshock region.

The foreshock is a highly dynamical region, hosting different kinds of kinetic transients. These include hot-flow anomalies (HFAs, Schwartz et al., 1985) and foreshock bubbles (FBs, Turner et al., 2013). The core of these transients is characterized by hot, tenuous plasma regions, in which flow deflection and pressure reduction occur. An impact of this pressure "hole" in the foreshock on the BS leads to an expansion of the magnetosphere followed by a compression (e.g., Sibeck et al., 1999; Turner et al., 2011; Archer et al., 2014, 2015). These impacts can also generate field-aligned currents and ultra-low frequency (ULF) waves in the magnetosphere and auroral brightening (Hartinger et al., 2013; Zhao et al., 2017; Wang et al., 2018; Liu et al., 2022).

Observations of phenomena like HFAs and FBs suggest that the reaction of the magnetosphere and the subsequent motion of the magnetopause (MP) happens on different scales. HFAs form when a solar wind discontinuity connects with the BS. The convective electric field has to point towards the discontinuity plane, accumulating back stream-

ing foreshock particles on one or both sides of the discontinuity (e.g., Schwartz et al., 2000). The core of the HFAs typically reaches transverse scale sizes of 1-2 R_E (Schwartz, 1995). As the core is convected with the discontinuity across the BS, the MP is distorted on a local scale (e.g. Sibeck et al., 1999; Turner et al., 2011). The cores of FBs form due to the concentration of foreshock ions upstream of discontinuities in the IMF (Liu et al., 2015, 2020). Simulation results suggest that FBs can reach scale sizes similar to the entire foreshock region, i.e., up to 10 R_E (Omidi et al., 2010, 2020). Spacecraft observations have confirmed that at least along the x-direction this is true (e.g. Liu, Turner, et al., 2016; Turner et al., 2020; Vu et al., 2022). These core sizes suggest a more global impact on the MP.

Archer et al. (2015) showed in a multi satellite case study, that FBs have indeed a global impact and lead to a large scale expansion of the MP across a transverse scale of $\sim$20 R_E (inferred from ground magnetometer data). However, Archer et al. (2015) could not infer whether the global expansion was due to the FB's transverse scale size or the fast transit of the solar wind discontinuity responsible for the FB across the BS. Vu et al. (2022) reported on a FB-like transient structure and inferred a scale size ~ 5 R_E across the BS surface. This suggests that the global response of the magnetosphere cannot be solely the result of the transverse scale.

In this paper we present recent observations of a large FB by the Magnetospheric Multi Scale (MMS) mission (Burch et al., 2016). The FB occurred on 23 December 2020 around 00:55 UT. Due to the conjunction with the three spacecraft of the Time History of Events and Macro-scale Interactions during Substorms (THEMIS) mission (Angelopoulos, 2008), the SOSMAG (Magnes et al., 2020; Constantinescu et al., 2020) magnetometer onboard the Geostationary-Korea Multi-Purpose Satellite-2A (GEO-KOMPSAT-2A) and one of the Geostationary Operational Environmental Satellites (GOES) at the geostationary orbit (GEO), we could study the FB and its impact at multiple locations in the magnetospheric system. We reevaluate the findings of Archer et al. (2015) and Vu et al. (2022) in regard to the transverse scale size of the FB, giving new constraints in multiple dimensions.

2 Data and Methods

For our analysis, we utilize a wide range of different spacecraft data: Magnetometer data with a 1 s cadence from the Advanced Composition Explorer (ACE, Stone et al., 1998; Smith et al., 1998) located far upstream at L1 around [217.57, -9.17, 17.16] R_E and time-shifted high resolution OMNI data (King & Papitashvili, 2005) are used to monitor upstream conditions of the solar wind. Burst mode data from the Fluxgate Magnetometer (MMS-FGM, Russell et al., 2016), the Fast Plasma Investigation (FPI, Pollock et al., 2016) experiment and the Fly's Eye Energetic Particle Spectrometer (FEEPS, Blake et al., 2016) on board of the MMS spacecraft are used for the analysis of the foreshock transient. We study the motion of the BS and MP with the Fluxgate Magnetometer data (TH-FGM, Auster et al., 2008) and particle data from the Electrostatic Analyzer (ESA, McFadden et al., 2008) of the three THEMIS spacecraft THA, THD, and THE. FGM and ESA data are used in the spin-resolution (FGM) and reduced mode (ESA) with cadences of about 3 to 4 s. We also utilize low resolution (fgl, 0.0625 s) FGM data from THA and THD for the whole event. Magnetic field data from SOSMAG (Magnes et al., 2020; Constantinescu et al., 2020) and GOES-17 (Loto'aniu et al., 2019) both with a data rate of 1 s are used to investigate the magnetospheric response.

All vector data are presented and analysed in the geocentric solar ecliptic (GSE) coordinate system. We assume that the positions of all spacecraft in these coordinates are quasi-stationary for the duration of the event, since the spacecraft are only moving at a few km/s, i.e., the distance travelled by the spacecraft is much smaller than the scale of the transient, since the event is only observed over a period of 30 min.

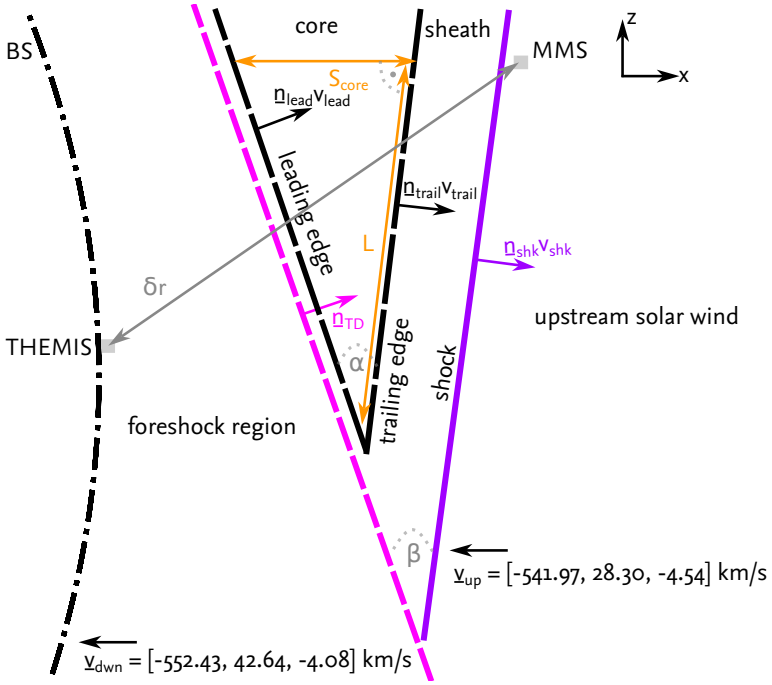

Figure 1. Schematic representation of the foreshock transient at the time MMS crosses the upstream shock, showing all important regions and boundaries. In addition, the estimates for the different scale sizes and the angles and distances required for the calculations are marked in orange and grey respectively.

For the classification of the foreshock transient in section 3.1 we use the criteria given by Turner et al. (2013, 2020) to distinguish between FB and HFA. We look at the boundaries, motion and trigger of the transient.

Similar to the method presented by Vu et al. (2022), we use a combination of minimum variance analysis (MVA, Sonnerup & Scheible, 1998) and the multi-spacecraft-timing method (MST, e.g., eq. 10.20 in Schwartz, 1998) to analyse the different boundaries of the FB and the magnetosphere. First we calculate normal directions with the MVA in a size varying window, which is slid across the whole event. We only consider normals for which the intermediate-to-minimum eigenvalue ratios are greater than 5 and time intervals capturing boundary or shock crossings entirely. For these preselected intervals and suitable spacecraft configurations (i. e., only for MMS), we also calculate the normals and boundary velocities with the MST method, and only consider normals which deviate less than 15° from the MVA results. The final normals are than calculated as a mean from all suitable intervals and given a standard deviation error.

We choose the sign of all calculated normal directions to point always in the upstream direction(i.e., with a positive x component) and adjust the sign of the boundary velocity accordingly (only necessary for MST results). The time differences between spacecraft observations required for the MST method, is calculated using cross correlation between each magnetic field components and calculating the mean from the three different time lags. Additionally, we also utilize the conservation of mass flux (CMF, eq. 10.29 in Schwartz, 1998) to calculate boundary velocities from the THEMIS and MMS MVA results to compare them, if applicable, with the MST velocities.

To determine the expansion speed v_{exp} of the transient and its core size perpendicular to the discontinuity plane S_{core} (see Fig 1), we follow Liu, Turner, et al. (2016)

and Turner et al. (2020):

$$v_{\rm exp} = |\underline{v}_{\rm dwn} \cdot \underline{n}_{\rm shk} - v_{\rm shk}|, \quad (1)$$

$$S_{\rm core} = |\underline{v}_{\rm dwn} \cdot \underline{n}_{\rm trail}| \Delta t_{\rm core}. \quad (2)$$

We compare the results with the equations given by Vu et al. (2022):

$$v_{\rm exp} = v_{\rm lead} + v_{\rm trail} - \underline{v}_{\rm dwn} \cdot (\underline{n}_{\rm lead} + \underline{n}_{\rm trail}), \quad (3)$$

$$S_{\rm core} = \frac{1}{2}(v_{\rm lead} + v_{\rm trail}) \Delta t_{\rm core}. \quad (4)$$

Here, $\underline{v}_{\rm dwn}$ is the downstream velocity vector measured by MMS, $\Delta t_{\rm core}$ is the amount of time (in s) that the spacecraft has spent in the transient core and the normal vectors $\underline{n}$ and boundary velocities v of the upstream shock, the leading inner boundary and the trailing inner boundary are denoted by $\underline{n}_{\rm shk}$ and $v_{\rm shk}$, $\underline{n}_{\rm lead}$ and $v_{\rm lead}$ and $\underline{n}_{\rm trail}$ and $v_{\rm trail}$, respectively. Fig. 1 visualizes the different regions, boundaries and vectors necessary for our analysis in a schematic depiction of a foreshock transient in the $x-z$-plane.

Assuming that the boundary planes of the transient are planar and extend beyond the observation points, we can calculate a point where the transient core should close as the intersection of the trailing and leading edge planes (similar to the estimation methode of Vu et al., 2022). The transverse scale $L_{\rm core}$ of the transient core can then be estimated from the distance between the intersection and the MMS position during the observation of the trailing boundary.

3 Observations

In Fig. 2 we present the location of the different spacecraft on 23 December 2020 between 00:40 and 01:10 in GSE coordinates. We use the time-shifted OMNI data, the Shue et al. (1998) MP model and the Chao et al. (2002) BS model to calculate the shown average location and shape of the MP and BS during the event.

MMS is located upstream of the BS in the solar wind around a mean position of [14.04, 7.52, 6.22] $R_{\rm E}$. The three THEMIS spacecraft are located roughly 2 $R_{\rm E}$ north of the subsolar point of the Chao et al. (2002) BS model, clustered around [12.94, 0.70, 2.27] $R_{\rm E}$ in the ion foreshock. MMS and THEMIS are roughly separated by 7.96 $R_{\rm E}$ (δr=[1.1 , 6.82, 3.95] $R_{\rm E}$). On GEO, SOSMAG is located around [4.89, -3.89, 2.16] $R_{\rm E}$ and GOES-17 around [3.22, 5.61, 1.33] $R_{\rm E}$. This configuration allows us to observe the transient event on a global scale across the dayside magnetosphere.

3.1 Solar wind and Foreshock - MMS observations

In Fig. 3 we present magnetic field and particle data of MMS1 sampled to a common cadence of 0.25 s. Additionally, we show the magnetometer data from ACE, time shifted by 44 min, which is roughly the time delay between the ACE and MMS positions. This timeshift will be justified later.

At 00:46:30 MMS crossed from a fast travelling solar wind ($v_{\rm MMS,dwn}$ = [-553.36, 41.99, -4.04] km/s) into the foreshock region of the Earth. Between 00:51 and 00:56, MMS encountered two strong flow deflections with v_x near and above 0 km/s. Accompanying these deflections are temperatures up to 10 times higher and ion densities noticeably lower than in the ambient solar wind. Upstream of the deflection, the spacecraft enters a region with high ion densities around 17 cm^{-3} and a strong dynamic pressure up to 10 nPa. After 00:58:30 the spacecraft is again located in the undisturbed solar wind. This signature clearly belongs to foreshock transients like an HFA or FB, characterized by a core region of hot tenuous plasma in which flow deflection and pressure reduction occur, bound by plasma sheath and an upstream shock (Turner et al., 2013).

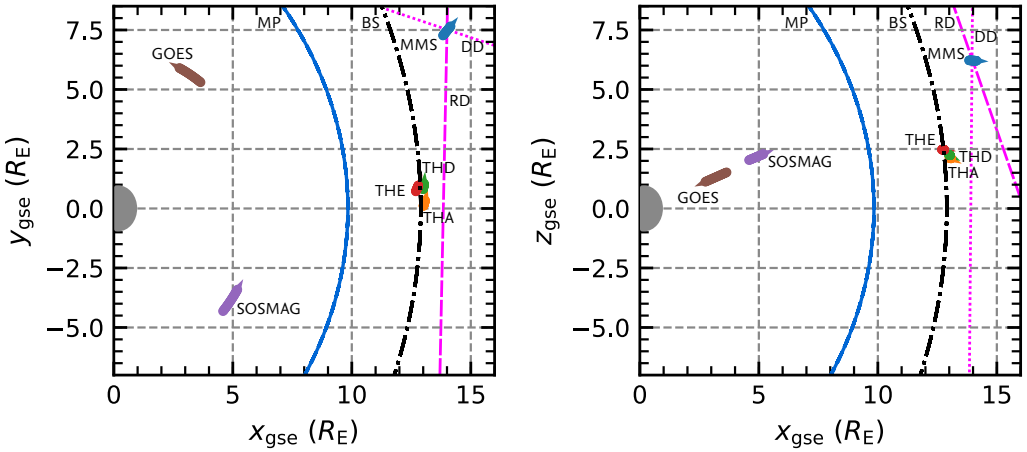

Figure 2. Spatial distribution of spacecraft on 23 December 2020 around 00:55 UT in the GSE x-y-plane (left panel) and x-z-plane (right panel), respectively. Earth is symbolised by the grey semicircle. The arrows at the spacecraft locations point along the spacecraft orbits. The Shue et al. (1998) model magnetopause and the Chao et al. (2002) model bow shock for $B_{z,\mathrm{IMF}} = -0.95$ nT, $p_{\mathrm{dyn}} = 2.55$ nPa, $\beta = 4.30$ and $M_{\mathrm{MS}} = 7.27$ are shown in blue and black, respectively. The discontinuities suspected to be responsible for the event are represented by a magenta dashed lines.

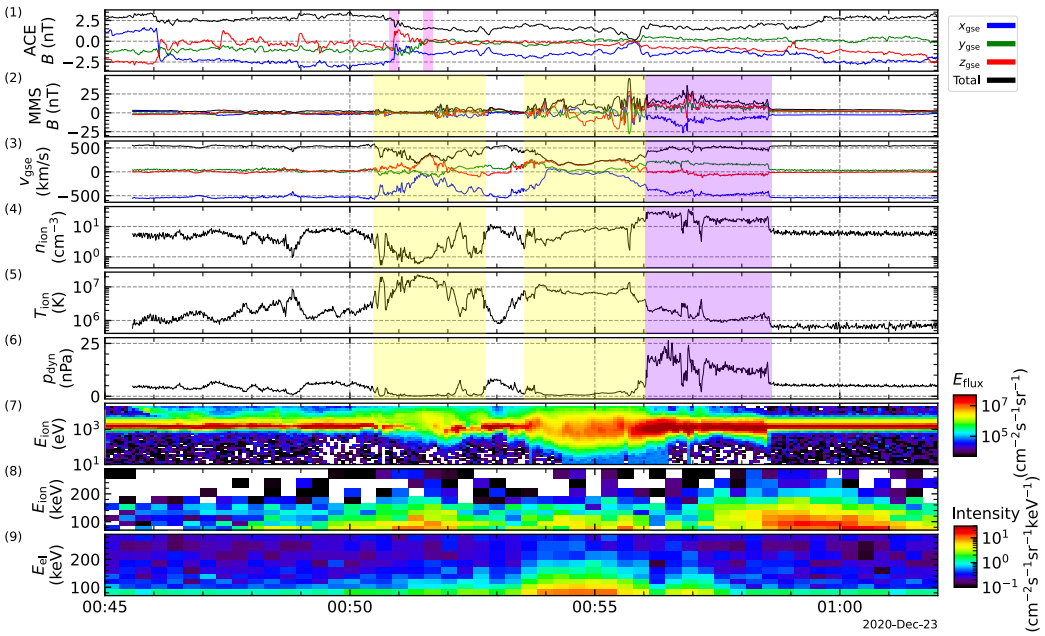

Figure 3. Time series plot of ACE and MMS1 data on 23 December 2020. From top to bottom the panels display the magnetic field data from ACE (44-min timeshifted), magnetic field data from MMS, the ion velocity, the ion density, the ion temperature, the dynamic pressure, the ion energy flux density and the high energetic ion and electron intensities. The coloured region indicate the core (yellow) and the upstream sheath and shock (violet) of the foreshock bubble. The magenta shaded region indicate two discontinuities observed by ACE.

Further evidence therefore comes from the FEEPS data. Both in the high energy electron and ion intensities (panels (8) and (9) of Fig. 3) we see spikes up to a energy regime of 200 keV limited to the core region of the transient between 00:54:00 and 00:56:00. Additionally, we also see high energy ions upstream of the event directly after the bounding upstream shock around 01:00:00. Highly energized particles are common in the core and upstream regions of transients, as they act as efficient particle accelerators (e.g., Wilson et al., 2016; Turner et al., 2018; Liu et al., 2019). Note that the energetic particles are not visible in the FPI data as they are obscured by the noise level of the instrument.

We propose that at least the signature between 00:54:00 and 00:58:30 belongs to an FB. In the following, we point out a few clear indicators that support our assumption:

1) The MMS spacecraft does not observe any features of a compression region (i.e. increased density and magnetic field strength) upon entry into either of the transient structures at 00:50:30 and 00:53:35 respectively. Such a compression region on the downstream side would be an clear indicator for HFAs.

2) The second transient shows an extended sheath region between its trailing inner boundary at 00:56 and the upstream shock edge around 00:58:30. The foot of this shock shows large amplitude waves, which is common for transients (e.g. Turner et al., 2020). The normal for the upstream shock calculated with the sliding MVA window with size varying between 4 s and 8 s yields [0.99, 0.05, -0.06] $\pm 0.51^\circ$. The normal calculated from the MST in the same intervals yields [0.99, 0.01, -0.14] $\pm 2.10^\circ$ with a shock velocity v_{shk} of -311.61 km/s roughly consistent with the results of -362.11 km/s from the CMF method. These normals show a very strong x component consistent for a FB shock expanding in sunward direction. The shock of a FB is usually a fast mode shock, i.e. the magnetic field should be coplanar across the shock and the MVA may not be reliable. Thus we also calculate a coplanarity estimate of the shock normal (see chapter 10.4.2 in Schwartz, 1998). This yields a normal of [0.94 , 0.19, -0.20] $\pm 14.98^\circ$ which agrees within 11.32° with the MST results.

3) Analysing the burst mode data with regard to the arrival time of the transient at the four MMS spacecraft, we can infer that the transient convects in negative x_{gse} direction, i.e. with the solar wind flow.

4) Foreshock transients typically form around or upstream of rotational (RD) or tangential (TD) discontinuities. However, the signature of the discontinuity in the spacecraft data (MMS) is often obscured by the foreshock transient signature. Therefore we look at the ACE data: We can identify multiple discontinuities in the ACE data. MVA with a window of width of 4 s to 60 s is performed on the discontinuities. With these normals we calculated a time delay of 35 to 40 minutes between observations at L1 and the arrival of the discontinuities at the MMS position using the method of Weimer et al. (2003). Still, this time shift give us only a rough estimate for the delay, thus we compared the the timeshifted ACE data with solar wind data from MMS (see Fig. 4). We can identify similar structures in these two time series, suggesting an additional timeshift of 4 min. Therefore, we suppose that the total timeshift should be 44 min. This time delay motivates the shift in the ACE data presented in Fig. 3. However, we want to point out, that each discontinuity has a unique time delay due to its orientation, and the presented timeshift should be viewed as an educated guess.

In panels 3 and 4 of Fig.4 we show the magnetic field cone and clock angle ($\vartheta_{\mathrm{cone}}$, $\vartheta_{\mathrm{clock}}$) for ACE and MMS. Comparing the MMS $\vartheta_{\mathrm{cone}}$ and $\vartheta_{\mathrm{clock}}$ downstream and upstream of the transients with the ACE angles (blue arrows in Fig.4), we can identify two discontinuities that seem to fit the observation of both transients at MMS (marked in magenta in Figs. 3 and 4). The analysis of the discontinuities yield a normal of [0.26, 0.97, -0.02] $\pm 1.13^\circ$ for the first and [0.95, -0.02, 0.30] $\pm 7.45^\circ$ for the second. According to Liu,

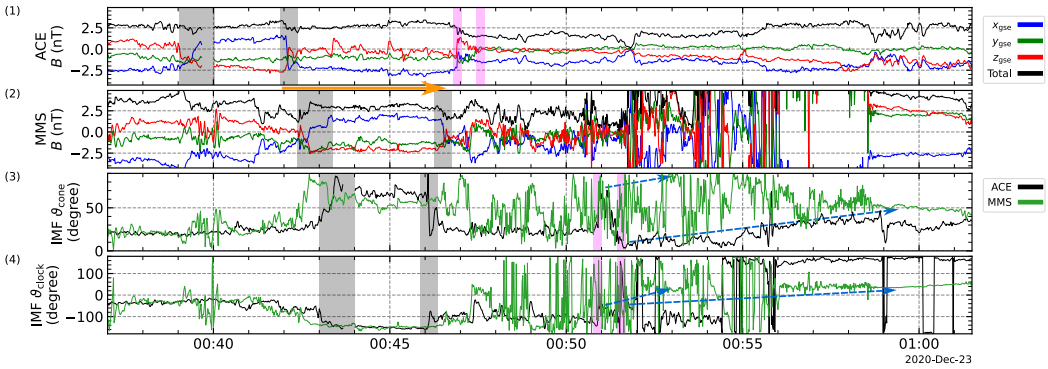

Figure 4. Time series plot of ACE and survey mode MMS1 data on 23 December 2020 in a 1 s resolution. The first panel shows ACE magnetic field data timeshifted by 40 min (details in the text). The second panel shows the MMS magnetic field data. The marked features in grey in the ACE and MMS magnetic field data suggest an additional timeshift (orange arrow) of ∼4 min. The IMF cone and clock angle are shown in the bottom panel for MMS and ACE (timeshifted with 44 min). The magenta shaded region mark the discontinuities responsible for the foreshock transients.

Turner, et al. (2016), we can classify the discontinuities utilizing the ratio of the normal component to the field magnitude (B_n/B) as follows: the second discontinuity yields $B_n/B = 0.87$, so it is most likely to be an RD type discontinuity, while the first discontinuity yields $B_n/B = 0.67$ and cannot be clearly classified as either an RD type or a TD type, so we can only refer to it as a directional discontinuity (DD). Overall, the second transient probably formed upstream or around the RD type solar wind discontinuity observed by ACE at 00:51:35 (already time shifted).

5) We calculate the solar wind convection electric fields downstream and upstream of the second transient from the MMS burst mode data. This yields electric fields of [0.10, 1.23, -0.65] mV/m downstream and [-0.13, -1.57, 0.97] mV/m upstream. Both vectors do not point back at the discontinuity plane of the upstream ACE discontinuity we suspect to be responsible. We have inferred this from the angles between the electric field vectors and the normal direction of the second ACE discontinuity, yielding 95.14° and 83.81° for the downstream and the upstream side, respectively.

These features, particularly those listed under (1), (2) and (5), are more likely to be characteristics of an FB than of an HFA. Thus, we identify the second foreshock transient as an FB which formed upstream of a RD type solar wind discontinuity and convects with the solar wind flow earthwards.

3.2 Bow shock and Magnetopause - THEMIS observations

In Fig. 5 we present TH-FGM and ESA data from the three THEMIS spacecraft. Shortly after MMS enters the core of the first transient, all THEMIS spacecraft cross the BS and encounter a strong sunward plasma flow in the magnetosheath between 00:50:30 and 00:52:30 (visible in THD and THA), indicating an outward moving BS. Additionally, MVA on the magnetic field data during the crossing yields [0.78, -0.49, -0.38] ±9.45° (THA), [0.25, 0.35, -0.90] ±6.60° (THD) and [0.20, 0.32, -0.93] ±2.56° (THE), hinting at a deformation of the BS (further extended in the northern hemisphere).

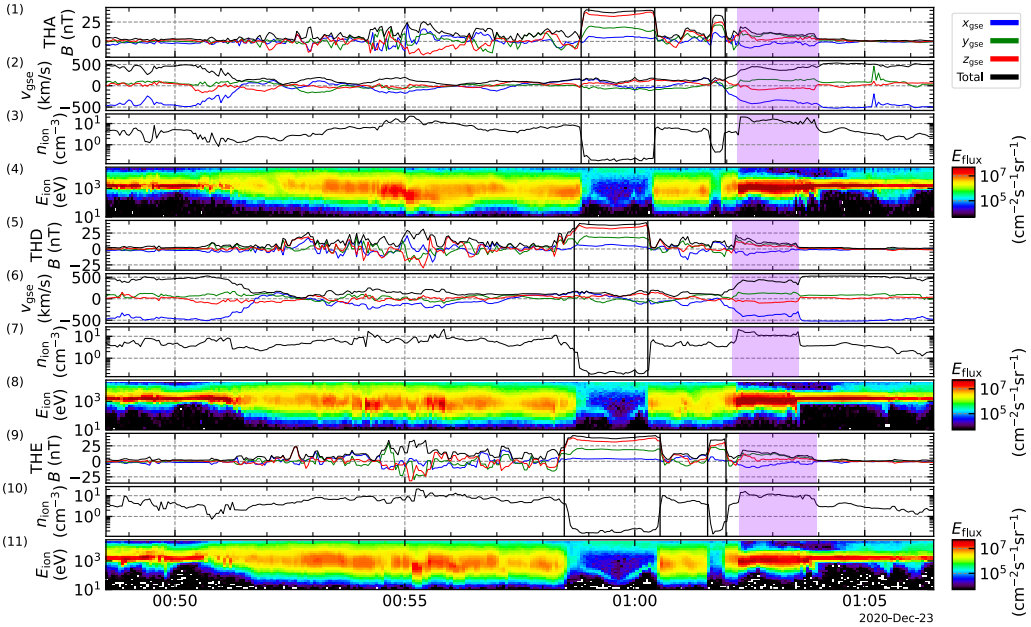

Figure 5. Time series plot of THEMIS data on 23 December 2020. From top to bottom the panels display the magnetic field data, ion velocity, ion density and the energy flux density for THA, THD and THE. Velocity data for THE is not available in a sufficient resolution and thus not plotted here. The black vertical lines indicate magnetopause crossings and the violet shaded region highlights the sheath region of the FB.

Starting with THE at 00:58:30 the spacecraft encounter a magnetopause crossing (MPC) and enter the magnetosphere, i.e., the magnetosphere expanded drastically such that the BS and MP both swept across the THEMIS spacecraft. We calculate an equivalent stand-off distance $R_{0,\mathrm{sc}}$ during this crossing using the Shue et al. (1998) MP model formula identical to the calculation done in Grimmich et al. (2023): $R_{0,\mathrm{sc}}$ is 12.95 R_{E} for THE the innermost probe, which is a deviation of 3.12 R_{E} to the prediction of the Shue et al. (1998) MP model (using OMNI data), confirming the extreme expansion. From MVA we get [0.80, -0.56, 0.20] ±5.22° (THA), [0.91, 0.22, -0.33] ±3.84° (THD) and [0.98, 0.16, -0.12] ±0.52° (THE) as normal directions. All of the normals show a strong x component, indicating that there is no local deformation, but rather a global motion of the MP. The associated boundary velocities from the CMF method are 100.16 km/s (THA) and 81.89 km/s (THD). For THE the velocity data is not useable, thus we can not calculate boundary velocities. However, they should be similar to THD's results as these two spacecraft are very close to each other.

After roughly 1 min all spacecraft cross back into the magnetosheath. Here, the MVA on the MPCs yields [0.88, -0.45, 0.11] ±4.73° (THA), [0.79, 0.51, -0.33] ±2.84° (THD) and [0.82, 0.45, -0.34] ±2.45° (THE) with velocities from the CMF method of -24.03 km/s (THA) and -74.19 km/s (THD). These values fit with an inward moving MP which seems to have an equilibrium position just inside the THEMIS orbits, as the boundary velocity drops from THD to THA.

Between 01:01:30 and 01:02:00 THA and THE encounter a second much shorter incursion into the magnetosphere. MVA yields [0.07, -0.87, 0.50] ±3.09° (THA) and [0.43, 0.64, -0.64] ±1.18° (THE) for the entry into the magnetosphere and [0.73, 0.44, -0.53] ±1.72° (THA) and [0.99, 0.10, -0.11] ±3.84° (THE) with a boundary velocity estimate

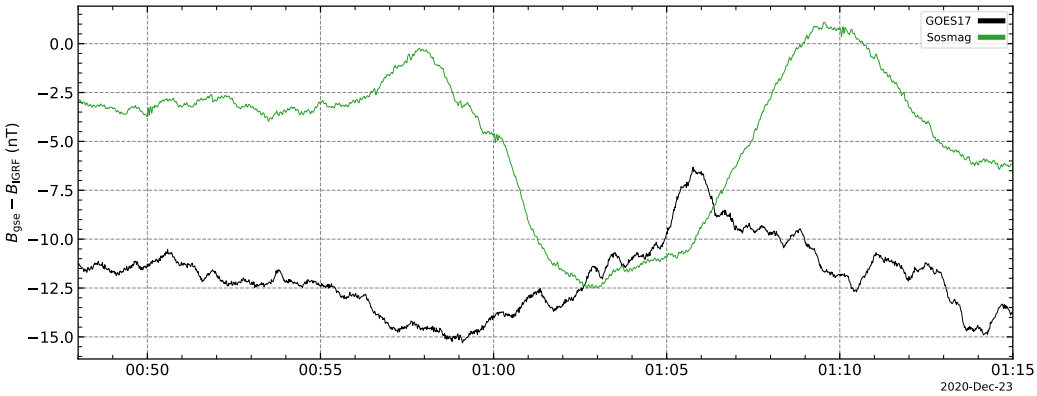

Figure 6. Time series plot of SOSMAG and GOES-17 total magnetic field data on 23 December 2020. The IGRF (Alken et al., 2021) at the spacecraft orbits is subtracted from the data.

from the CMF method for THA of 11.42 km/s and -203.27 km/s, respectively. These values indicate a rapid compression of the magnetosphere after a slow outward motion, which stems from the reaction of the MP to a new equilibrium position.

Additionally, we can observe that the plasma velocity has a strong sunward component during the first magnetopause crossing (MPC) and a more anti sunward component during or shortly after the second MPC. This observation also fits with the interpretation of an expanding MP followed by a compression of the MP for both magnetosphere incursions.

We also see that, between 01:02:20 and 01:04:00, all three spacecraft encounter a sheath region which looks very similar to parts of the sheath region of the FB (marked in purple in Fig. 5). Correlation analysis of the total magnetic field from MMS1 and THEMIS reveals a correlation coefficient of 0.73 for THA and THD and a coefficient of 0.83 for THE in this sheath region. Thus, we can infer that THEMIS encountered the sheath region of the FB and then crosses into the pristine solar wind. Additionally the calculated MVA normals for the fgl data of THD and THA of the upstream shock of the sheath are [0.92, -0.05, -0.39] ±3.08° and [0.96, -0.08, -0.25] ±4.55° for THA and THD. These normals lie within 15.31° of the normal we calculated for the upstream shock of the FB on MMS data. Again, we used the coplanarity estimate for the normal direction as a more reliable estimate of the shock normal yielding [0.92, 0.26, -0.27] ±8.71° and [0.89, 0.40, -0.21] ±4.93° for THA and THD, respectively. This results agree roughly with the MVA results and within 23.6° with the estimates of the MMS observation. In the fgl data (not shown) a shock foot with large amplitude waves similar to the MMS observations is visible as well. The CMF method yields 289.50 km/s (THA) and 307.40 km/s (THE) for the shock velocity.

3.3 Magnetospheric response - GEO observations

The total magnetic field of the SOSMAG and GOES observations is displayed in Fig. 6. We subtract the magnitude of the IGRF model (Alken et al., 2021) at both spacecraft locations to better visualize the variations in the magnetospheric field. Both time series show a clear decrease in the magnitude over several minutes followed by a strong increase of the field. The signature is first observed at GOES-17 and a few minutes later also by SOSMAG. However, the signature in the SOSMAG data is much clearer and stronger, and we can see a short increase of the field preceding the decrease.

These signatures are fitting for a large expansion followed by a compression of the magnetosphere, as magnetic field strength should decrease in an expansion and increase when the magnetic field is more compressed. The first magnetic field increase in the SOSMAG data also hints at a compression preceding the expansion.

We also checked the Disturbance Storm-Time Index D_{st} (Nose et al., 2015), which indicates how much the magnetic field is disturbed by the ring current. During the event the hourly D_{st} index is -3 nT, i. e., no strong ring current activity is responsible for the observed deviation in the magnetic field.

4 Discussion

From the MMS observation, we could clearly identify the transient signature as an FB forming upstream of an RD, preceded by an unidentified transient forming upstream of another discontinuity. The first transient is likely to be an early-stage transient, as neither edge shows the compression region associated with late-stage FB and HFA-like transients. Further investigation is required to clearly identify this transient. In the following we focus more on the FB and its impact on the magnetospheric system.

For the estimate of the FB size we calculate normal directions and boundary velocities for the leading and the trailing inner edges of the FB at 00:54:00 and 00:56:00, respectively. For the leading edge, MVA yields [0.28, 0.90, 0.34] $\pm 0.46^\circ$ with a velocity from the CMF method of -194.32 km/s, while MST in the same interval yields [0.37, 0.89, 0.26] $\pm 2.41^\circ$ with a velocity estimate of -212.30 km/s. For the trailing edge, MVA yields [0.89, 0.46, -0.11] $\pm 0.40^\circ$ with a velocity from CMF method of -266.79 km/s, while MST in the same interval yields [0.96, 0.25, -0.11] $\pm 2.52^\circ$ with a velocity estimate of -250.50 km/s.

Utilizing eq. (3) and (4) we calculate an expansion speed for the FB core of 224.68 km/s and a size Score perpendicular to the RD of 10.39 R_E. Eq. (1) and (2) yield an expansion speed of 234.30 km/s and a core size of 11.91 R_E. These results are in agreement with previously reported expansion speeds and sizes of FBs (Liu, Turner, et al., 2016; Turner et al., 2020; Vu et al., 2022).

Our estimation for the transverse scale yields $L_{\text{core}} = 7.58\ R_E$ using the distance from MMS to the intersection point of the edge planes. Since the FB is basically a 2D structure in the x-z plane that extends in the y direction, this estimation is done in the $y = 0$ plane. This transverse scale estimation is clearly a lower limit, since the FB can be extended beyond the observation point MMS and close at another location.

Interestingly, the sheath of this FB seems to be very large, as MMS is inside this region for multiple minutes (00:56:00 to 00:58:30). The reason for this large sheath region could be the age of the FB which we estimate to be roughly 4 min by dividing the core size by the expansion speed (Liu, Turner, et al., 2016; Turner et al., 2020). Hence, the FB probably formed 21 R_E upstream of MMS and is in its late stage of expansion when MMS observes its features.

Since we can see the sheath and shock edges of the FB in the THEMIS observations, the expansion of the magnetosphere is most likely caused by the FB. The interaction between the BS and the FB is also probably responsible for the observed bow shock distortions. The FB shock edge begins to replace the BS, then the FB is still a few R_E away from the magnetosphere, leading to an expansion and distortion of the original BS towards the FB. This fits with the observation of the BS crossing at THEMIS even before the FB is observed at MMS. Although, the unidentified transient could also be responsible for the distortion of the BS as the orientation of the first discontinuity suggest a connection of discontinuity with the BS at the time MMS observed the first transient, which would also cause the BS motion.

The time delay of the FB discontinuity from the MMS position to THEMIS is roughly 3 to 4 min, again calculated with the method described in Weimer et al. (2003). This agrees with our assumption as MMS enters the core of the FB at 00:54:00 and the first MPC at THEMIS is observed around 00:58:30. The low dynamic pressure in the FB core causes the magnetosphere to expand rapidly, which leads to an MP moving fast and overshooting the actual equilibrium position. This can be inferred from the high boundary velocities at the first MPC between 80 km/s and 100 km/s and then the very different velocities at the second MPC. Furthermore, THA and THE observe a second crossing into the magnetosphere which indicates an oscillating MP resulting from such an initial overshoot. We infer the equilibrium position of the MP to be just earthward of the THE location.

For an estimation of the equivalent stand-off distance of the MP $R_{0,\mathrm{eq}}$ in the equilibrium position, we use the simple pressure balance formula (e.g. Baumjohann & Treumann, 1997)

$$\frac{R_{0,\mathrm{eq}}}{R_\mathrm{E}} = \sqrt[6]{\frac{2(g_1^0)^2}{\mu_0 \kappa p_\mathrm{dyn}}}. \tag{5}$$

Here, the Earth's dipole coefficient is $g_1^0 = 30,000$ nT and κ=0.88. With a dynamic pressure of roughly 0.4 nPa in the FB's core, $R_{0,\mathrm{eq}}$ yields 12.64 R_E agreeing nicely with the derived equivalent stand-off distance of 12.95 R_E for the THE MPCs, and our assumption. The Shue et al. (1998) model prediction for the stand-off distance of 9.75 R_E also agrees with the results from eq. (5) yielding 9.31 R_E when using p_dyn values from MMS solar wind observations before the event. We can summarize that the FB led to a massive MP displacement of more than 3 R_E, which is to our knowledge the largest reported displacement of the MP caused by an FB.

The timing between the observations of MMS and THEMIS also allows us to give another estimate for the transverse scale of the FB. While THEMIS observes the first MPC (i.e., the FB has reached the THEMIS position), MMS encounters the upstream shock edge of the FB. Thus, the FB has to cover at least the distance between the two spacecraft constellations, and δr projected on the FB shock plane can be used as a low limit estimate for the transverse scale size of this event. This would lead to an estimate of roughly 7.94 R_E.

MMS also sees energetic ions upstream of the FB. Based on the pitch angle spectra (not shown), those ions move sunward away from the FB shock, which could hint at a foreshock region associated with the FB (Liu, Hietala, et al., 2016). Following the method used in Liu, Hietala, et al. (2016), we can estimate the velocity of the reflected ion beam: We utilize the upstream solar wind velocity v_up = [-541.97, 28.30, -4.54] km/s and the IMF vector B_up = [-2.68, 2.16, 1.78] nT from MMS observations at 01:01:00 to calculate the Hoffmann-Teller velocity for the FB shock:

$$v_\mathrm{HT} = \frac{n_\mathrm{shk} \times ((v_\mathrm{up} - v_\mathrm{shk}) \times B_\mathrm{up})}{n_\mathrm{shk} \cdot B_\mathrm{up}}. \tag{6}$$

Subsequently, the reflected ion beam of the FB foreshock can be estimated with

$$v_\mathrm{r,FB} = -v_\mathrm{up} + 2(v_\mathrm{shk} + v_\mathrm{HT}). \tag{7}$$

Eq. 7 yields a velocity of [127.03, 297.73, 287.10] km/s. From the FEEPS data we estimate that the FB foreshock is roughly observed for 2.5 min. Thus, the size of the foreshock along the FB shock surface direction n_shk should be roughly 10.19 R_E, stemming from reflected ion beam velocity and the observation time. The size of the foreshock also indicates typically the shock surface size, i.e. the transverse scale of the FB. Hence, we have another estimate for this scale which roughly agrees with our previous estimates.

All together, we can constrain the size if this FB to be 10-12 R_E in x and 7-10 R_E in the transverse (y-z) direction. As far as we know, this is the largest estimate of an

FB size in the y or z GSE dimensions. Previous studies only have given constraints in the x dimension (Turner et al., 2020) or found only values up to 5.1 R_E (Vu et al., 2022). Our estimates together with constraints given for the x dimension fully support the original predictions of Omidi et al. (2010), namely that the size of the FB is ~ 10 R_E in the x and y dimensions.

Due to the magnetic field observations at GEO we can infer that the magnetosphere is impacted by the FB on a global scale. However, the structure clearly impacts the dusk side before the dawn side, as GOES-17 observed the response to the event before SOSMAG, and with a smaller amplitude. The timing of the observation of GOES-17 is fitting with the observation of the first unidentified transients which could be responsible for an initial response of the magnetosphere. At this point in time the FB probably is only starting to interact with the BS leading to a smaller response. When the FB is connected over its whole transverse scale with the BS, the magnetosphere fully expands in a large and strong response, as can be seen in the THEMIS and shortly afterwards in the SOSMAG data. The first compression in the SOSMAG data might also stem from the unidentified transient, i.e., this transient also plays a role in the response of the magnetosphere. Therefore, we suppose that the impact of FB's, as predicted by simulations (Omidi et al., 2010) and previously observed (Archer et al., 2015), occurs on a global scale but is not instantaneous on the whole dayside. The enormous scale leads to an initial global distortion that follows the motion of the transient across the dayside and leads to a response in other parts of the magnetosphere.

Additionally, we can infer more constraints in regard to the expansion of the FB during this event. As predicted by Omidi et al. (2010) the FB shock edge becomes the new BS, when hitting the original BS. We can verify this, as THEMIS observed basically the shock edge of the FB after the last MPCs instead of a normal BS before entering the solar wind. Using the CMF method we calculate shock velocities for THA and THD for the FB shock and find -289.50 km/s and -307.40 km/s, respectively. With eq. (1) these boundary velocities lead to expansion speeds of 219.28 km/s (THA) and 225.32 km/s (THD) for the FB. These expansion speeds are clearly similar to the ones observed at MMS reaffirming that both constellations observed the same shock at different locations. These results also suggest that the expansion of the FB seems to be constant over the 5 min which lie between the MMS and THEMIS observations. However, as we already mentioned, the BS and the FB's shock merge together, thus the expansion speeds might not be solely stemming from the FB expansion and could also already contain parts of the BS motion.

5 Summary and Conclusions

We report the impact of a large foreshock transient on the magnetospheric system on 23 December 2020. Different spacecraft either observed this transient directly or the response of the magnetosphere to it. We identify this transient as a large and also quite matured foreshock bubble forming upstream of a tangential discontinuity.

The scattered spacecraft allow us to determine the transverse scale of the foreshock bubble in different ways, which lies probably between 7 and 10 R_E. This result agrees nicely with predictions from simulations and succeeds previous estimates for this scale size.

We can also clearly infer that the transient leads to a more than 3 R_E displaced magnetopause and triggers a global response in the magnetospheric field, as expected. We suppose that this global response stems from a combination of the transverse scale of the foreshock bubble and its motion across the dayside of magnetospheric system. The scale results in a huge distortion, which is then moved through the magnetosphere and is triggering the observed global response, gradually.

In a statistical analysis of MP locations that deviate from MP model predictions, Grimmich et al. (2023) found that favourable solar wind conditions for extreme MP locations are similar to the conditions associated with the occurrence of foreshock transients (high solar wind speeds with large Alfvén Mach numbers), suggesting that these transients may be a reason for the deviation from model predictions. Our study is a confirmation of this, as we have identified an FB to be the origin of one extreme MP displacement happening while the solar wind velocity was 550 km/s with a Alfvén Mach number of 15.

This event might also offer the opportunity to study the formation of a foreshock corresponding to the shock edge of the foreshock bubble in more detail in the future, as we find energetic ions upstream of the bubble. Furthermore, the transient we discuss here in detail is not the only one occurring on this day; many more transients are observed in a short period of time. These might allow to further investigate the response of the magnetosphere to the arrival of such transients.

Open Research Section

All spacecraft data used is publicly available and can be accessed via the open source Python Space Physics Environment Data Analysis Software (pySPEDAS) which can be found here: `https://github.com/spedas/pyspedas`. The Dst index used in this paper was provided by the WDC for Geomagnetism, Kyoto `http://wdc.kugi.kyoto-u.ac.jp/wdc/Sec3.html`.

Acknowledgments

We are grateful for the dedicated efforts and support of the entire MMS mission team, including development, science operations, and the Laboratory of Atmospheric and Space Physics, Science Data Center (LASP, SDC) at the University of Colorado, Boulder. We acknowledge NASA contract NAS5-02099 and V. Angelopoulos for use of data from the THEMIS Mission. Specifically: C. W. Carlson and J. P. McFadden for use of ESA data and K. H. Glassmeier, U. Auster and W. Baumjohann for the use of FGM data provided under the lead of the Technical University of Braunschweig and with financial support through the German Ministry for Economy and Technology and the German Center for Aviation and Space (DLR) under contract 50OC 0302. SOSMAG data is made available via ESA's Space Safety Programme and its provision forms part of the ESA Space Weather Service System. The National Oceanic and Atmospheric Administration (NOAA) provides the space weather data of GOES. We thank J. King and N. Papitashvili of the National Space Science Data Center (NSSDC) in the NASA/GSFC for the use of the OMNI 2 database, and also N. Ness and D. McComas for the use of the ACE data. FP and JZDM are supported by the Deutsches Zentrum für Luft- und Raumfahrt (DLR) under contract 50OC2201. The authors want to thank Nick Hatzigeorgiu and Eric Grimes for the ongoing development of PySPEDAS. TZL, FB and MOA acknowledge the support by the International Space Science Institute (ISSI) in Bern through ISSI International Team project #465.

References

Alken, P., Thébault, E., Beggan, C. D., Amit, H., Aubert, J., Baerenzung, J., ... Zhou, B. (2021, dec). International Geomagnetic Reference Field: the thirteenth generation. *Earth, Planets and Space*, *73*(1), 49. doi: 10.1186/s40623-020-01288-x

Angelopoulos, V. (2008, apr). The THEMIS Mission. *Space Sci. Rev.*, *141*(1-4), 5-34. doi: 10.1007/s11214-008-9336-1

Archer, M. O., Turner, D. L., Eastwood, J. P., Horbury, T. S., & Schwartz, S. J.

(2014, oct). The role of pressure gradients in driving sunward magnetosheath flows and magnetopause motion. *Journal of Geophysical Research (Space Physics)*, *119*(10), 8117-8125. doi: 10.1002/2014JA020342

Archer, M. O., Turner, D. L., Eastwood, J. P., Schwartz, S. J., & Horbury, T. S. (2015, feb). Global impacts of a Foreshock Bubble: Magnetosheath, magnetopause and ground-based observations. *Planetary and Space Science*, *106*, 56-66. doi: 10.1016/j.pss.2014.11.026

Auster, H. U., Glassmeier, K. H., Magnes, W., Aydogar, O., Baumjohann, W., Constantinescu, D., ... Wiedemann, M. (2008, dec). The THEMIS Fluxgate Magnetometer. *Space Sci. Rev.*, *141*(1-4), 235-264. doi: 10.1007/s11214-008-9365-9

Baumjohann, W., & Treumann, R. (1997). *Basic Space Plasma Physics*. Imperial College Press.

Blake, J. B., Mauk, B. H., Baker, D. N., Carranza, P., Clemmons, J. H., Craft, J., ... Westlake, J. (2016, mar). The Fly's Eye Energetic Particle Spectrometer (FEEPS) Sensors for the Magnetospheric Multiscale (MMS) Mission. *Space Sci. Rev.*, *199*(1-4), 309-329. doi: 10.1007/s11214-015-0163-x

Burch, J. L., Moore, T. E., Torbert, R. B., & Giles, B. L. (2016, mar). Magnetospheric Multiscale Overview and Science Objectives. *Space Sci. Rev.*, *199*(1-4), 5-21. doi: 10.1007/s11214-015-0164-9

Chao, J. K., Wu, D. J., Lin, C. H., Yang, Y. H., Wang, X. Y., Kessel, M., ... Lepping, R. P. (2002, jan). Models for the Size and Shape of the Earth's Magnetopause and Bow Shock. In L.-H. Lyu (Ed.), *Space weather study using multipoint techniques* (p. 127).

Constantinescu, O. D., Auster, H.-U., Delva, M., Hillenmaier, O., Magnes, W., & Plaschke, F. (2020, December). Maximum-variance gradiometer technique for removal of spacecraft-generated disturbances from magnetic field data. *Geoscientific Instrumentation, Methods and Data Systems*, *9*(2), 451-469. doi: 10.5194/gi-9-451-2020

Grimmich, N., Plaschke, F., Archer, M. O., Heyner, D., Mieth, J. Z. D., Nakamura, R., & Sibeck, D. G. (2023, aug). Study of Extreme Magnetopause Distortions Under Varying Solar Wind Conditions. *Journal of Geophysical Research (Space Physics)*, *128*(8), e2023JA031603. doi: 10.1029/2023JA031603

Hartinger, M. D., Turner, D. L., Plaschke, F., Angelopoulos, V., & Singer, H. (2013, jan). The role of transient ion foreshock phenomena in driving Pc5 ULF wave activity. *Journal of Geophysical Research (Space Physics)*, *118*(1), 299-312. doi: 10.1029/2012JA018349

King, J. H., & Papitashvili, N. E. (2005, feb). Solar wind spatial scales in and comparisons of hourly Wind and ACE plasma and magnetic field data. *Journal of Geophysical Research (Space Physics)*, *110*(A2), A02104. doi: 10.1029/2004JA010649

Liu, T. Z., An, X., Zhang, H., & Turner, D. (2020, oct). Magnetospheric Multiscale Observations of Foreshock Transients at Their Very Early Stage. *The Astrophysical Journal*, *902*(1), 5. doi: 10.3847/1538-4357/abb249

Liu, T. Z., Angelopoulos, V., & Lu, S. (2019, jul). Relativistic electrons generated at Earth's quasi-parallel bow shock. *Science Advances*, *5*(7), eaaw1368. doi: 10.1126/sciadv.aaw1368

Liu, T. Z., Hietala, H., Angelopoulos, V., & Turner, D. L. (2016, may). Observations of a new foreshock region upstream of a foreshock bubble's shock. *Geophysical Research Letters*, *43*(10), 4708-4715. doi: 10.1002/2016GL068984

Liu, T. Z., Turner, D. L., Angelopoulos, V., & Omidi, N. (2015, oct). THEMIS observations of tangential discontinuity-driven foreshock bubbles. *Geophysical Research Letters*, *42*(19), 7860-7866. doi: 10.1002/2015GL065842

Liu, T. Z., Turner, D. L., Angelopoulos, V., & Omidi, N. (2016, jun). Multipoint observations of the structure and evolution of foreshock bubbles and their rela-

tion to hot flow anomalies. *Journal of Geophysical Research (Space Physics)*, *121*(6), 5489-5509. doi: 10.1002/2016JA022461

Liu, T. Z., Wang, C.-P., Wang, X., Angelopoulos, V., Zhang, H., Lu, X., & Lin, Y. (2022, nov). Magnetospheric Field-Aligned Current Generation by Foreshock Transients: Contribution by Flow Vortices and Pressure Gradients. *Journal of Geophysical Research (Space Physics)*, *127*(11), e2022JA030700. doi: 10.1029/2022JA030700

Loto'aniu, T. M., Redmon, R. J., Califf, S., Singer, H. J., Rowland, W., Macintyre, S., ... Todirita, M. (2019, jun). The GOES-16 Spacecraft Science Magnetometer. *Space Sci. Rev.*, *215*(4), 32. doi: 10.1007/s11214-019-0600-3

Magnes, W., Hillenmaier, O., Auster, H. U., Brown, P., Kraft, S., Seon, J., ... Lee, C. H. (2020, October). Space Weather Magnetometer Aboard GEO-KOMPSAT-2A. *Space Sci. Rev.*, *216*(8), 119. doi: 10.1007/s11214-020-00742-2

McFadden, J. P., Carlson, C. W., Larson, D., Ludlam, M., Abiad, R., Elliott, B., ... Angelopoulos, V. (2008, dec). The THEMIS ESA Plasma Instrument and In-flight Calibration. *Space Sci. Rev.*, *141*(1-4), 277-302. doi: 10.1007/s11214-008-9440-2

Nose, M., Iyemori, T., Sugiura, M., & Kamei, T. (2015). *Geomagnetic Dst index* [dataset]. World Data Center for Geomagnetism, Kyoto. Retrieved from `https://isds-datadoi.nict.go.jp/wds/10.17593_14515-74000.html` doi: 10.17593/14515-74000

Omidi, N., Eastwood, J. P., & Sibeck, D. G. (2010, jun). Foreshock bubbles and their global magnetospheric impacts. *Journal of Geophysical Research (Space Physics)*, *115*(A6), A06204. doi: 10.1029/2009JA014828

Omidi, N., Lee, S. H., Sibeck, D. G., Turner, D. L., Liu, T. Z., & Angelopoulos, V. (2020, sep). Formation and Topology of Foreshock Bubbles. *Journal of Geophysical Research (Space Physics)*, *125*(9), e28058. doi: 10.1029/2020JA028058

Pollock, C., Moore, T., Jacques, A., Burch, J., Gliese, U., Saito, Y., ... Zeuch, M. (2016, mar). Fast Plasma Investigation for Magnetospheric Multiscale. *Space Sci. Rev.*, *199*(1-4), 331-406. doi: 10.1007/s11214-016-0245-4

Russell, C. T., Anderson, B. J., Baumjohann, W., Bromund, K. R., Dearborn, D., Fischer, D., ... Richter, I. (2016, mar). The Magnetospheric Multiscale Magnetometers. *Space Sci. Rev.*, *199*(1-4), 189-256. doi: 10.1007/s11214-014-0057-3

Schwartz, S. J. (1995, apr). Hot flow anomalies near the Earth's bow shock. *Advances in Space Research*, *15*(8-9), 107-116. doi: 10.1016/0273-1177(95)00025-A

Schwartz, S. J. (1998, jan). Shock and Discontinuity Normals, Mach Numbers, and Related Parameters. In G. Paschmann & P. W. Daly (Eds.), *Analysis methods for multi-spacecraft data* (Vol. 1, p. 249-270). ISSI Scientific Reports Series, ESA/ISSI.

Schwartz, S. J., Chaloner, C. P., Christiansen, P. J., Coates, A. J., Hall, D. S., Johnstone, A. D., ... Woolliscroft, L. J. C. (1985, nov). An active current sheet in the solar wind. *Nature*, *318*(6043), 269-271. doi: 10.1038/318269a0

Schwartz, S. J., Paschmann, G., Sckopke, N., Bauer, T. M., Dunlop, M., Fazakerley, A. N., & Thomsen, M. F. (2000, jun). Conditions for the formation of hot flow anomalies at Earth's bow shock. *Journal of Geophysical Research*, *105*(A6), 12639-12650. doi: 10.1029/1999JA000320

Shue, J. H., Song, P., Russell, C. T., Steinberg, J. T., Chao, J. K., Zastenker, G., ... Kawano, H. (1998, aug). Magnetopause location under extreme solar wind conditions. *Journal of Geophysical Research*, *103*(A8), 17691-17700. doi: 10.1029/98JA01103

Sibeck, D. G., Borodkova, N. L., Schwartz, S. J., Owen, C. J., Kessel, R., Kokubun,

S., ... Zastenker, G. N. (1999, mar). Comprehensive study of the magnetospheric response to a hot flow anomaly. *Journal of Geophysical Research*, *104*(A3), 4577-4594. doi: 10.1029/1998JA900021

Smith, C. W., L'Heureux, J., Ness, N. F., Acuña, M. H., Burlaga, L. F., & Scheifele, J. (1998, jul). The ACE Magnetic Fields Experiment. *Space Sci. Rev*, *86*, 613-632. doi: 10.1023/A:1005092216668

Sonnerup, B. U. Ö., & Scheible, M. (1998, jan). Minimum and Maximum Variance Analysis. In G. Paschmann & P. W. Daly (Eds.), *Analysis methods for multispacecraft data* (Vol. 1, p. 185-220). ISSI Scientific Reports Series, ESA/ISSI.

Stone, E. C., Frandsen, A. M., Mewaldt, R. A., Christian, E. R., Margolies, D., Ormes, J. F., & Snow, F. (1998, jul). The Advanced Composition Explorer. *Space Sci. Rev.*, *86*, 1-22. doi: 10.1023/A:1005082526237

Turner, D. L., Eriksson, S., Phan, T. D., Angelopoulos, V., Tu, W., Liu, W., ... Glassmeier, K. H. (2011, apr). Multispacecraft observations of a foreshock-induced magnetopause disturbance exhibiting distinct plasma flows and an intense density compression. *Journal of Geophysical Research (Space Physics)*, *116*(A4), A04230. doi: 10.1029/2010JA015668

Turner, D. L., Liu, T. Z., Wilson, L. B., Cohen, I. J., Gershman, D. G., Fennell, J. F., ... Burch, J. L. (2020, jul). Microscopic, Multipoint Characterization of Foreshock Bubbles With Magnetospheric Multiscale (MMS). *Journal of Geophysical Research (Space Physics)*, *125*(7), e27707. doi: 10.1029/2019JA027707

Turner, D. L., Omidi, N., Sibeck, D. G., & Angelopoulos, V. (2013, apr). First observations of foreshock bubbles upstream of Earth's bow shock: Characteristics and comparisons to HFAs. *Journal of Geophysical Research (Space Physics)*, *118*(4), 1552-1570. doi: 10.1002/jgra.50198

Turner, D. L., Wilson, L. B., Liu, T. Z., Cohen, I. J., Schwartz, S. J., Osmane, A., ... Burch, J. L. (2018, sep). Autogenous and efficient acceleration of energetic ions upstream of Earth's bow shock. *Nature*, *561*(7722), 206-210. doi: 10.1038/s41586-018-0472-9

Vu, A., Liu, T. Z., Zhang, H., & Pollock, C. (2022, feb). Statistical Study of Foreshock Bubbles, Hot Flow Anomalies, and Spontaneous Hot Flow Anomalies and Their Substructures Observed by MMS. *Journal of Geophysical Research (Space Physics)*, *127*(2), e2021JA030029. doi: 10.1029/2021JA030029

Wang, B., Nishimura, Y., Hietala, H., Shen, X.-C., Shi, Q., Zhang, H., ... Weatherwax, A. (2018, aug). Dayside Magnetospheric and Ionospheric Responses to a Foreshock Transient on 25 June 2008: 2. 2-D Evolution Based on Dayside Auroral Imaging. *Journal of Geophysical Research (Space Physics)*, *123*(8), 6347-6359. doi: 10.1029/2017JA024846

Weimer, D. R., Ober, D. M., Maynard, N. C., Collier, M. R., McComas, D. J., Ness, N. F., ... Watermann, J. (2003, jan). Predicting interplanetary magnetic field (IMF) propagation delay times using the minimum variance technique. *Journal of Geophysical Research (Space Physics)*, *108*(A1), 1026. doi: 10.1029/2002JA009405

Wilson, L. B., Sibeck, D. G., Turner, D. L., Osmane, A., Caprioli, D., & Angelopoulos, V. (2016, nov). Relativistic Electrons Produced by Foreshock Disturbances Observed Upstream of Earth's Bow Shock. *Physical Review Letters*, *117*(21), 215101. doi: 10.1103/PhysRevLett.117.215101

Zhao, L. L., Zhang, H., & Zong, Q. G. (2017, jun). Global ULF waves generated by a hot flow anomaly. *Geophysical Research Letters*, *44*(11), 5283-5291. doi: 10.1002/2017GL073249